Mechanism of self-excitation of terahertz plasma oscillations in periodically double-gated electron channels

2008 J. Phys.: Condens. Matter 20 384207

(http://iopscience.iop.org/0953-8984/20/38/384207)

IOP PUBLISHING JOURNAL OF PHYSICS: CONDENSED MATTER

J. Phys.: Condens. Matter **20** (2008) 384207 (6pp) doi:10.1088/0953-8984/20/38/384207

Mechanism of self-excitation of terahertz plasma oscillations in periodically double-gated electron channels

V Ryzhii[1], A Satou[1], M Ryzhii[1], T Otsuji[2] and M S Shur[3]

[1] Computer Solid State Physics Laboratory, University of Aizu, Aizu-Wakamatsu 965-8580, Japan
[2] Research Institute of Electrical Communication, Tohoku University, Sendai 980-8577, Japan
[3] Department of Electrical, Computer, and Systems Engineering, Rensselaer Polytechnic Institute, Troy, NY 12180, USA

E-mail: v-ryzhii@u-aizu.ac.jp

Received 9 March 2008, in final form 21 April 2008
Published 21 August 2008
Online at stacks.iop.org/JPhysCM/20/384207

Abstract

We develop a device model for a heterostructure device with an electron channel and with a periodic system of interdigitated gates. Using this model, we find the conditions of the self-excitation of plasma oscillations in portions of the channel. It is shown that the self-excitation of plasma oscillations in these devices and the terahertz emission observed in the experiments (Otsuji *et al* 2006 *Appl. Phys. Lett.* **89** 263502; Meziani *et al* 2007 *Appl. Phys. Lett.* **90** 061105; Otsuji *et al* 2007 *Solid-State Electron.* **51** 1319) might be attributed to the electron-transit-time effect in the barrier regions.

1. Introduction

Recently, the emission of terahertz radiation was observed from a heterostructure device with an electron channel similar to a field-effect transistor with an interdigitated system of gates [1]. A schematic view of the device structure is shown in figure 1(a). At the applied gate voltages, the electron channel is partitioned into the strips of a two-dimensional electron gas (2DEG) beneath the positively biased gates and the barrier regions, separating these 2DEG strips, beneath the negatively biased gates. The terahertz emission from this device was attributed to the self-excitation of the plasma oscillations in the 2DEG strips and the conversion of these oscillations into radiative electro-magnetic modes. However, the mechanism of the self-excitation of the plasma modes, i.e. the mechanisms of instability of a steady-state current flow from the device source to the drain when some source–drain voltage is applied is not understood yet. As shown in the experiments [1–3], the illumination of optical light at the device, which causes the interband photogeneration of electrons and holes, promotes the emission of the terahertz radiation. Previously, several mechanisms of the plasma instability leading to the self-excitation of the plasma oscillations in the heterostructures akin to field-effect transistors have been proposed and substantiated theoretically and experimentally: the Dyakonov-Shur mechanism of the plasma oscillation self-excitation [4, 5], mechanisms associated with the negative dynamic conductivity (due to the negative differential conductivity in the case of the resonant tunneling [6] or the electron-transit-time effects [7, 8]) of some portions of device structures, the resonant excitation of the plasma oscillations by incoming optical radiation of two lasers with close frequencies [9–12]. In this paper, we develop a model for the heterostructure device with the periodically double-gated electron channel and propose a plausible mechanism which can be responsible for the plasma instability leading to the terahertz emission from such a device [1–3]. This mechanism is associated with the electron-transit-time effects due to the finiteness of the electron transit time across the barrier regions separating the 2DEG strips. On the basis of the model developed, we provide realistic interpretation of the experimental results [1–3].

2. Device model

We consider a heterostructure with an electron channel and a periodic system of interdigitated gates, as shown in figure 1(a). The gate lengths are L_{g1} and L_{g2} and the period of the gate system is $L > (L_{g1}+L_{g2})$. It is assumed that the bias potentials

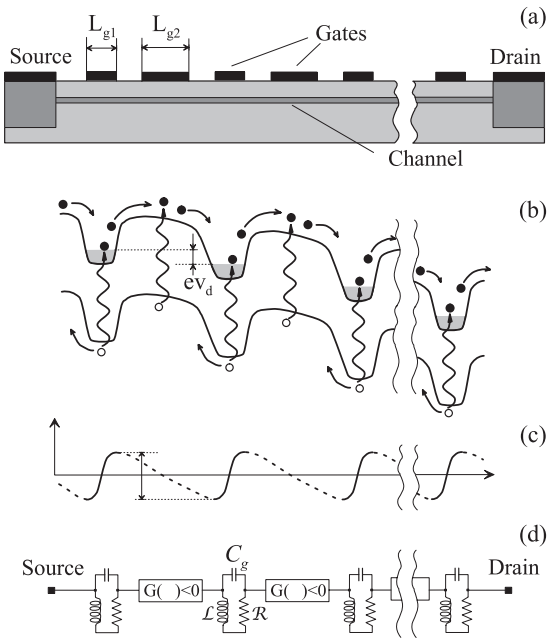

Figure 1. Schematic view of a heterostructure with schematic view of (a) the device structure, (b) its band diagram, (c) snapshot of spatial distribution of the ac potential associated with plasma oscillations, and (d) simplified equivalent circuit of the device. Opaque and open circles correspond to electrons and holes, respectively. Wavy arrows indicate photogeneration of electrons and holes.

are applied to the pertinent gates: a positive (with respect to the channel pinch-off voltage) potential V_{g1} is applied to the short gates (with the length L_{g1}) and a negative potential $V_{g2} < 0$ to the longer gates. As a result, the dc electron density under the former gates is equal to $\Sigma_0 = \Sigma_d + æ V_{g1}/4\pi e W_g = æ(V_{g1} - V_{off})/4\pi e W_g$, where Σ_d is the donor sheet density in the electron channel (or in the gate layer), e is the electron charge, æ is the dielectric constant, W_g is the gate layer thickness, and V_{off} is the channel pinch-off voltage. The value $|V_{g2}|$ is assumed to be sufficiently large, so that the portions of the electron channel under the long gates are depleted. The length of the depleted section (barrier length) is $L_b \simeq L - L_{g1}$. Thus, the electron system in the device under consideration comprises the strips of 2DEGs (under short gates) separated by the potential barriers formed under long depleting gates. Under a small source–drain voltage V_d, a lateral dc current created by electrons overcoming the barriers occurs. The band diagram for the electron channel is shown schematically in figure 1(b).

Let us search for the signal component of the self-consistent potential in the form $\delta\varphi(x,t) = \delta\varphi_\omega(x)\exp(-i\omega t)$, where ω is the signal frequency. In this case, the self-consistent potential and the signal component of the electron density $\Sigma_\omega(x)$ in the portions of the electron channel under the positively biased gates, i.e. in the quasi-neutral portions of the electron channel $(-L_{g1}/2 + nL < x < L_{g1}/2 + nL)$, are related by the following equation:

$$\delta\varphi_\omega = -\frac{4\pi e W_g}{æ}\delta\Sigma_\omega. \tag{1}$$

Here $n = 0, \pm1, \pm2, \ldots$ is the index of the gate.

The linearized hydrodynamic equations (the Euler equation and the continuity equation) coupled with (1) result in the following equation for the signal component of the potential in the quasi-neutral portions of the electron channel [5, 6]:

$$s^2\frac{d^2\delta\varphi_\omega}{dx^2} + \omega(\omega + i\nu)\delta\varphi_\omega = 0. \tag{2}$$

Here $s = \sqrt{4\pi e^2\Sigma_0 W_g/æm}$ is the characteristic plasma velocity in the gated electron channel, m is the electron effective mass, and ν is the collision frequency of electrons with impurities and phonons.

3. Dispersion equation for plasma oscillations

The signal components of the potential at the points separating the quasi-neutral and depleted sections of the channel should be matched taking into account the ac currents between the neighboring quasi-neutral sections (see figure 1(c), where the solid and dashed lines correspond to the ac potential distributions in 2DEG strips and in the barrier regions, respectively). Assuming that these currents are associated with the thermionic emission over the barriers in the depleted sections, it is necessary to calculate the ac current between two neighboring 2DEG strips (the ac conductance $G(\omega)$ in figure 1(d)), taking into account the presence of the highly conducting gate covering the depletion region and the finiteness of the electron transit time. According to the Shockley–Ramo theorem [13, 14], the ac current between two neighboring 2DEG strips can be calculated as the ac current injected from one 2DEG strip into the depletion region multiplied by a complex phase factor $f(\theta)$ depending on the so-called transit angle $\theta = \omega\tau_t/2$, where τ_t is the characteristic electron transit time, and determined by the geometry of the conducting parts of the system. Considering this, one can use the following equation:

$$\delta j_\omega = j_m \exp\left(\frac{\eta e v_d - \Delta_b}{k_B T}\right)\left(\frac{\eta e\Delta\varphi_\omega}{k_B T}\right) f\left(\frac{\omega\tau_t}{2}\right)$$
$$= j_0\left(\frac{\eta e\Delta\varphi_\omega}{k_B T}\right) f\left(\frac{\omega\tau_t}{2}\right). \tag{3}$$

Here, Δ_b is the height of the barrier in the depleted sections without the dc source–drain bias and the signal variations of the potential, $v_d = V_d/N$ is the dc potential drop across each barrier, N is the number of periods of the gate system, k_B is the Boltzmann constant and T is the temperature, $j_m = e\Sigma_0 v_{th}$ is the maximum current which can exist between the sections in question, $j_0 = j_m \exp[(\eta e v_d - \Delta_b)/k_B T]$ is the dc current, and $v_{th} \simeq \sqrt{k_B T/m}$ is the thermal velocity. The value $\eta \leqslant 1/2$ is determined by the shape of the barrier. If $L_{g2} \gg W_g$, $\eta \simeq l_g/L \ll 1$. The phase factor can be presented as

$$f\left(\frac{\omega\tau_t}{2}\right) = \frac{1}{L_{eff}}\int_0^{L_{eff}} dx\, g(x)\exp\left(i\frac{\omega\tau_t x}{L_{eff}}\right), \tag{4}$$

where L_{eff} is the effective length of the electron transit (between highly conducting parts of the device), and $g(x)$ is a geometrical form factor. In the cases of the electron

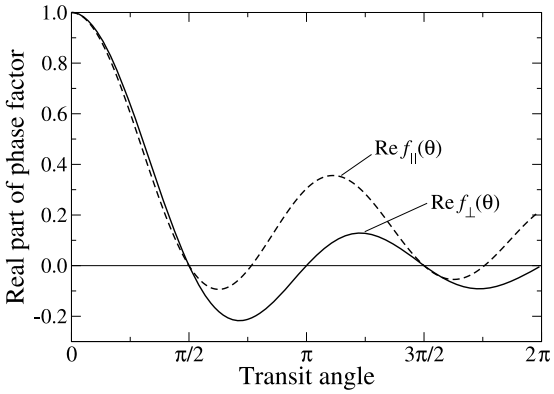

Figure 2. Real parts of the phase factors as functions of the electron transit angle θ.

propagation between two parallel conducting planes (as in the usual capacitor) and two coplanar conducting planes, $g(x) = 1$ and $g(x) = L_{\rm eff}/\sqrt{L_{\rm eff}^2 - x^2}$, respectively [15].

Integrating over the coordinate x in (4), for the two cases in question one can obtain the following, respectively [15]:

$$f_{\perp}(\theta) = {\rm e}^{{\rm i}\theta}\frac{\sin\theta}{\theta}, \qquad f_{\parallel}(\theta) = {\rm e}^{{\rm i}\theta}J_0(\theta), \tag{5}$$

where $J_0(\theta)$ is the Bessel function of zero order. In the system under consideration, the depleting gate substantially affects the ac conductance between the 2DEG strips. To avoid rather numerical calculations, we shall assume that the electrons injected from one 2DEG strip and collected by another contribute to the ac induced current only during their flight between the 2DEG strips and edges of the gate. In this case, one can set the effective length equal to $L_{\rm eff} \sim l_{\rm g} = L - L_{\rm g1} - L_{\rm g2}$, i.e. of the order of the spacing between the gates. This assumption is supported by the experimental fact that the properties of the systems under consideration with significantly different lengths of the depleting gates but equal space between the neighboring gates are fairly similar. Hence, $\tau_{\rm t} = l_{\rm g}/v_{\rm t}$, and $\theta = \omega\tau_{\rm t}/2 = \omega l_{\rm g}/2v_{\rm th}$. Both functions in (5) provide similar dependences of the phase factor on the transit angle and can be considered as the extreme limits for the real dependence. Figure 2 shows the dependences of the real parts of $f_{\perp}(\theta)$ and $f_{\parallel}(\theta)$, which are important in the following.

On the other hand, the ac current is equal to the ac conductivity current in the quasi-neutral section near its edge $x = L_{\rm g1}/2$, which is proportional to the lateral ac electric field $-{\rm d}\varphi_\omega/{\rm d}x$ at this point:

$$\delta j_\omega = -\frac{e^2\Sigma_0}{m(\nu - {\rm i}\omega)}\frac{{\rm d}\delta\varphi_\omega}{{\rm d}x}\bigg|_{x=\pm L_{\rm g1}/2}. \tag{6}$$

The ac potential drop, $\Delta\varphi_\omega$, across the barrier located between $x = L_{\rm g1}/2$ and $x = L - L_{\rm g1}/2$ is given by (see figure 1(c)):

$$\Delta\varphi_\omega = \delta\varphi|_{x=L_{g1}/2}\delta\varphi|_{x=L-L_{\rm g1}/2}. \tag{7}$$

For simplicity, we assume that the velocity of the electrons propagating over the barrier is of the order of the thermal velocity. Similar relations can be written down for other barrier regions.

For the plasma oscillations modes with asymmetrical distributions of the ac potential under the short gates, $\delta\varphi|_{x=L-L_{\rm g1}/2} = -\delta\varphi|_{x=L_{\rm g1}/2}$. Hence, (7) can be presented as

$$\Delta\varphi_\omega = \pm 2\delta\varphi|_{x=\pm L_{\rm g1}/2}. \tag{8}$$

Thus, equalizing the right-hand sides of (3) and (6) and considering (8), the boundary condition for (2) can be represented as follows:

$$\frac{{\rm d}\delta\varphi_\omega}{{\rm d}x}\bigg|_{x=\pm L_{\rm g1}/2} = \pm{\rm i}2\eta\nu\tau_{\rm th}\left(\frac{j_0}{j_{\rm m}}\right)\left(\frac{\omega + {\rm i}\nu}{\nu}\right) \times f\left(\frac{\omega\tau_{\rm t}}{2}\right)\frac{\delta\varphi_\omega}{l_{\rm g}}\bigg|_{x=\pm L_{\rm g1}/2}. \tag{9}$$

As a result, searching for the solution of (2) in the region $-L_{\rm g1}/2 \leqslant x \leqslant L_{\rm g1}/2$ in the form

$$\delta\varphi_\omega \propto \sin\left[\frac{\sqrt{\omega(\omega + {\rm i}\nu)}\,x}{s}\right] \tag{10}$$

and taking into account boundary condition (9), we obtain the following dispersion equation which determines the complex signal frequency ω, i.e. the spectrum of the plasma oscillations and the rate of their growth or damping:

$$\sqrt{\frac{\omega}{\omega + {\rm i}\nu}}\cot\left[\frac{\pi\sqrt{\omega(\omega + {\rm i}\nu)}}{2\Omega}\right] = {\rm i}\beta\left(\frac{j_0}{j_{\rm m}}\right)f\left(\frac{\omega\tau_{\rm t}}{2}\right), \tag{11}$$

where

$$\Omega = \frac{\pi s}{L_{\rm g1}} = \sqrt{\frac{4\pi^3 e^2\Sigma_0 W_{\rm g}}{æ m L_{\rm g1}^2}} \tag{12}$$

is the characteristic plasma frequency and $\beta = 2\eta s/v_{\rm th}$.

4. Plasma instability

If the height of the barriers in the depleted sections of the channel is sufficiently large, so that $\beta(j_0/j_{\rm m}) \ll 1$, the right-hand side of (11) is very small. In the lowest approximation, one can set it equal to zero. In this case, (11) yields the following formula for the complex signal frequency: $\omega = \Omega_k - {\rm i}\nu/2$, where $\Omega_k = \Omega(2k - 1)$ and $k = 1, 2, 3, \ldots$ is the plasma mode index. Thus, at high barriers the quasi-neutral sections are effectively separated from each other and the plasma frequencies ${\rm Re}\,\omega = \Omega_k$ and the plasma oscillations growth rate, i.e. the imaginary part of the signal frequency ${\rm Im}\,\omega = \gamma_k$, is negative: $\gamma_k = -\nu/2$. This implies that, in such a case, the plasma oscillations under consideration are damped out.

At lower barriers, the term in the right-hand side of (11) becomes essential. In this case, one can search for solutions of (11) in the form $\omega = \Omega_k + \delta$, where $|\delta|$ is assumed to be small in comparison with Ω. As a result, we obtain

$$\gamma_k \simeq -\frac{\nu}{2}\left[1 + \frac{4\beta}{\pi}\left(\frac{\Omega}{\nu}\right)\left(\frac{j_0}{j_{\rm m}}\right){\rm Re}\,f\left(\frac{\Omega_k\tau_{\rm t}}{2}\right)\right]. \tag{13}$$

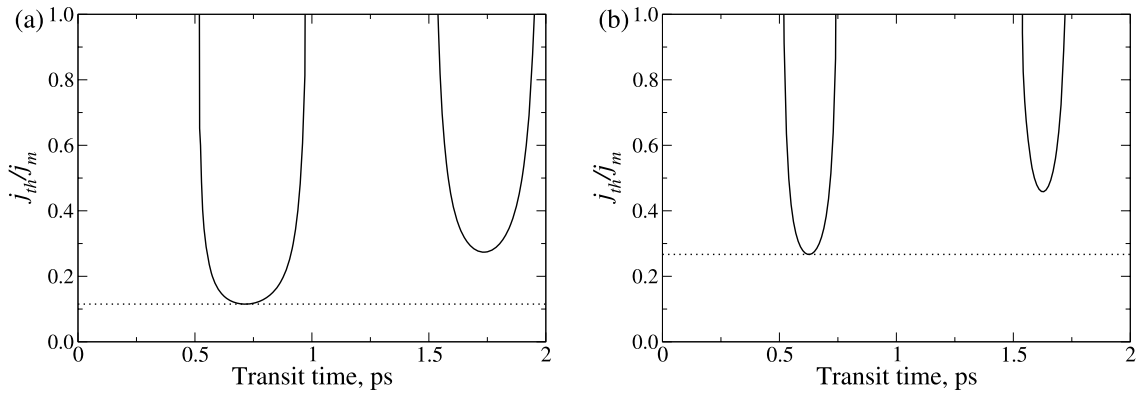

Figure 3. Normalized instability threshold current $j_{\rm th}/j_{\rm m}$ versus transit time $\tau_{\rm t}$ calculated for different form factors ((a) for Re $f_\perp(\theta)$ and (b) for Re $f_\parallel(\theta)$) with $k = 1$ and $\Omega/2\pi = 2$ THz. The dotted lines depict $j_{\rm th}^{\rm min}/j_{\rm m}$.

When Re $f(\Omega_k\tau_{\rm t}/2) < 0$, the second term in the brackets in (13) associated with the electron-transit-time effects is negative. This occurs at some values of the transit angle $\Omega_k\tau_{\rm t}/2$ and implies that the plasma oscillations growth rate can be positive. Using (13), we arrive at the following conditions at which the plasma oscillations growth rate $\gamma_k > 0$:

$$\frac{\nu}{\Omega} < \frac{4a\beta}{\pi}\left(\frac{j_0}{j_{\rm m}}\right), \tag{14}$$

where a is a numerical coefficient equal to $|\,{\rm Re}\, f(\theta)|$ at the first minimum of Re $f(\theta)$. At the first minimum Re $f_\perp(\theta) = \cos\theta\sin\theta/\theta \simeq -0.217$ and Re $f_\parallel(\theta) = J_0(\theta)\cos\theta \simeq -0.094$, hence the coefficient a depends on the device geometry: $0.094 < a < 0.217$. At relatively high barriers or low temperatures ($\Delta_{\rm b} > k_{\rm B}T$), inequality (14) is satisfied when the quality factor of the plasma oscillations $Q \sim \Omega/\nu$ is sufficiently large. If condition (14) is satisfied, the electron system in the device under consideration is electrically unstable. This instability corresponds to the self-excitation of the plasma oscillations modes for which $\Omega_k\tau_{\rm t} \sim 2.5\pi$. The necessary condition of the plasma oscillation self-excitation can be expressed via the dc current j_0:

$$j_0 > j_{\rm th}^{\rm min} = j_{\rm m}\left(\frac{\pi}{8\eta a}\right)\left(\frac{\nu}{\Omega}\right)\left(\frac{v_{\rm th}}{s}\right). \tag{15}$$

At $\eta = 0.25$, the factor $(\pi/8\eta a) = 7.24$–16.7. The last two factors in the right-hand side of (15) are usually fairly small, so that $j_{\rm th}$ is small in comparison with $j_{\rm m}$, i.e. the plasma instability can occur at the dc current j_0 which is smaller than the current maximum value $j_{\rm m}$. Considering the dependences of Ω and s on the dc electron density Σ_0, the minimum threshold current can also be presented as

$$j_{\rm th}^{\rm min} = b\left(\frac{L_{\rm g1}}{W_{\rm g}}\right)\left(\frac{m\nu v_{\rm th}^2}{e}\right), \tag{16}$$

where $b = (æ/32\pi\eta a)$. Assuming æ $= 12$ and $\eta = 0.25$, for the factor b in (16) we obtain $b \simeq 2.2 - 5.1$. Setting $m = 4\times 10^{-29}$ g, $\nu = 10^{12}$ s^{-1}, $v_{\rm th} \simeq 2\times 10^7$ cm s^{-1}, $s = 10^8$ cm s^{-1}, $L_{\rm g1}/W_{\rm g} = 2$, $L_{\rm g1} = 250$ nm (with these, $\Omega/2\pi = 2$ THz), we find $j_{\rm th}^{\rm min} \simeq 48$–$112$ mA cm^{-1}, and inequality (15) becomes $j_0 > (0.12 - 0.27)\,j_{\rm m}$. These quantities are of the same order as those observed in the experiments [1–3].

The value $j_{\rm th}^{\rm min}$ corresponds to the transit time $\tau_{\rm t}$ at which the factor Re $f(\Omega_k\tau_{\rm t}/2)$ reaches the absolute minimum. For other values of $\tau_{\rm t}$ (at which Re $f(\Omega_k\tau_{\rm t}/2) < 0$), the real threshold current $j_{\rm th}$ is given by

$$j_{\rm th} = j_{\rm th}^{\rm min}\frac{\min\ {\rm Re}\, f(\Omega_k\tau_{\rm t}/2)}{{\rm Re}\, f(\Omega_k\tau_{\rm t}/2)}. \tag{17}$$

Figure 3 shows the dependence of the normalized instability threshold current $j_{\rm th}/j_{\rm m}$ on the transit time $\tau_{\rm t}$ calculated for different phase functions ((a) for Re $f_\perp(\theta)$ and (b) for Re $f_\parallel(\theta)$) with $k = 1$ and $\Omega/2\pi = 2$ THz. The dotted lines in figure 3 depict $j_{\rm th}^{\rm min}/j_{\rm m}$. Since the growth rate γ_k can be positive only when Re $f(\theta) < 0$ and the current j_0 cannot exceed the maximum current $j_{\rm m}$, the plasma oscillation instability ($\gamma_k > 0$) can occur with some ranges of the transit time, as seen in figure 3.

Figure 4 shows the values of the plasma oscillation growth rate $\gamma_k/2\pi$ ($k = 1$) as a function of the transit time $\tau_{\rm t}$ at different values of the dc current $j_0/j_{\rm m}$ with the above-mentioned device parameters. One can see from figure 4 that the plasma instability can occur at some ranges of the transit time if the current is sufficiently large.

5. Discussion

As follows from the above plasma instability criterion (see (15)), an increase in the source–drain voltage $V_{\rm d}$ (and, consequently, in the value $v_{\rm d}$) can lead to the transition from a stable state to the plasma oscillations self-excitation. The transition from a stable state to the self-excitation of the plasma oscillations due to the plasma instability is accompanied by an increase in the dc current j_0 above its threshold value $j_{\rm th}$. The emission of terahertz radiation observed previously [1–3] might be attributed to the transformation of the self-excited plasma oscillations in the device with periodic gates considered above into transverse electro-magnetic modes.

An increase in the source–drain voltage can result in a sub-linear increase in the dc current due to heating of electrons

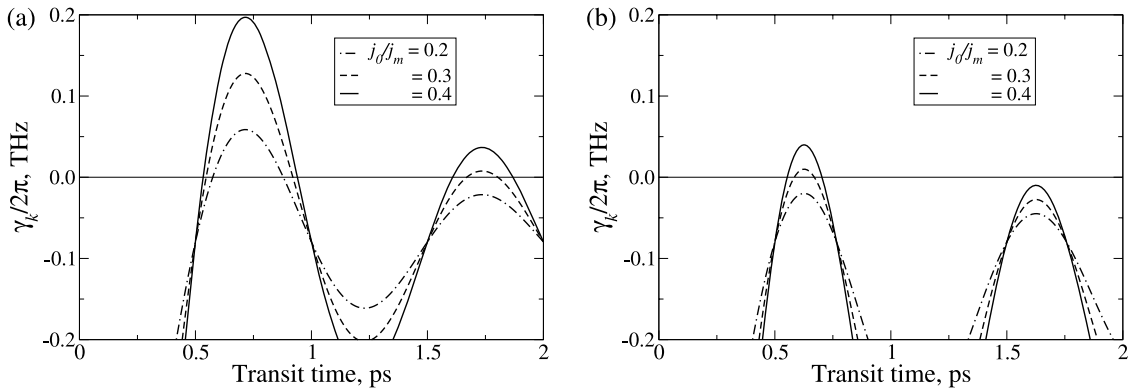

Figure 4. Plasma oscillations growth rate $\gamma_k/2\pi$ ($k = 1$) as a function of transit time τ_t with $j_0/j_m = 0.2, 0.3, 0.4$ for different form factors (device parameters mentioned in the text are used). ((a) for Re $f_\perp(\theta)$ and (b) for Re $f_\parallel(\theta)$).

in the 2DEG strips and, consequently, an increase in the thermionic emission of electrons from one strip to another.

The illumination of the device under consideration by light resulting in the interband photogeneration of electrons and holes should also promote the plasma instability and the terahertz emission. The mechanism of the effect of illumination is associated with the accumulation of the photogenerated holes in the barrier regions (see figure 1(b)) and, hence, the lowering of these barriers. The sensitivity of the plasma instability to the variation of the source–drain voltage and illumination was observed experimentally. The equations obtained above can also be used in the case of illumination, bearing in mind that the value of the dc current j_0 crucial for the instability condition (see (17) and (18)) increases compared with that in the dark conditions:

$$j_0 = j_0^{\text{dark}} + \mathcal{R}I. \tag{18}$$

Here $\mathcal{R} \propto \gamma/\tau_r$ is the device photoresponsivity and I is the flux of the incident optical radiation, where γ is the quantum efficiency of optical absorption and τ_r is the recombination time (the lifetime of holes in the barrier regions). The latter can be fairly long due to a spatial separation of holes (located mainly in the barrier regions) and electrons (located mainly in the 2DEG strips). This can provide rather high values of the photoresponsivity due to large photoelectric gain. Such an effect is common for the photoconductivity in different inhomogeneous semiconductor structures [16–18] (see also [19]) for example, in heavily doped strongly compensated semiconductors and the so-called dual-band quantum-well photodetectors. Owing to a relatively long recombination time, the elevated values of the dc current and, therefore, the favored conditions for the plasma instability and terahertz emission can be maintained not only at stationary illumination but during a prolonged period after the optical pulses.

Due to a drop in the potential along the structure associated with the applied source–drain voltage, the dc electron densities in different 2DEG strips Σ_0 can be slightly different. As a result, the pertinent values of the characteristic plasma frequency Ω corresponding to different 2DEG strips can differ from each other. Taking into account that the plasma instability in question can occur in a certain range of the transit angles, where Re $f < 0$ (see (13)), the spread in the plasma frequencies can be responsible for the relatively wide spectrum of the emitted terahertz radiation. The excitation of plasma oscillations and the pertinent terahertz emission with a substantially narrow spectrum was observed in the devices under consideration when the generation of photoelectrons and photoholes was due to short optical pulses. In the framework of our model, the effect of narrowing of the spectrum can be attributed to the fact that strong optical pulses provide more uniform distributions of the electron density over the different 2DEG strips, because in such a case the electron densities in these strips during some period after the excitation are determined to a greater extent by the photogeneration. As shown previously [20–24], the distribution of the dc potential in a multiple-well structure under illumination can be smoother in the main portion of the structure (except a narrow region adjacent to the source contact). Moreover, the shape of the dc potential distributions in multiple-well structures and in the device under consideration depends on the properties of the source contact. Hence, the spectrum of plasma oscillations and emitted terahertz radiation can be different in the devices with thermionic injection from the source contact (as schematically shown in figure 1(b)) and with tunneling injection from this contact. One needs to point out that the excitation of the plasma oscillations modes with a nonuniform distribution along the 2DEG strips (in the direction perpendicular to the current flow) can markedly complicate the pattern of the effect [25]. However, this requires a separate careful study.

The mechanism of the plasma instability under consideration and the pertinent self-excitation of the plasma oscillations can also be explained using the simplified device equivalent circuit shown in figure 1(d). In this circuit, $C_g \propto æ L_{g1}/W_g$ is the capacitance of the 2DEG strip, $R \propto m\nu/\Sigma_0$ is its resistance, and $\mathcal{L} \propto mL_{g1}/\Sigma_0$ is the inductance of this strip associated with the electron inertia [8], so that $\Omega = (C\mathcal{L})^{-1/2}$. The barrier region conductance $G(\omega) = \delta j_\omega/\Delta\varphi_\omega \propto j_0$. It is a function of the signal frequency ω and is negative in certain ranges of this frequency corresponding to the electron-transit-time resonances. The $C - \mathcal{L} - R$ sections of the circuit play the role of the resonators, which are excited due to the negative

dynamic conductance of the barrier regions which electrically connect such resonators.

One might concede that the emission of optical phonons by the electrons propagating across the barrier region can also be responsible for the plasma instability and terahertz radiation. Such mechanisms of plasma instability have been discussed for a rather long time [26–28]. However, the dc potential drop, ev_d, across each barrier region in some devices studied experimentally was less than 20 meV, so that the energy acquired by electrons in these region is markedly smaller than the optical phonon energy $\hbar\omega_0$.

6. Conclusions

We proposed a device model for a heterostructure device with the periodically double-gated electron channel. The model accounts for the features of the electron transport across the device structure with the 2DEG strips separated by the barrier regions and the possibility of the plasma oscillations in the 2DEG strips electrically coupled via the barrier regions. We demonstrated that, due to the negative dynamic conductance of the barrier regions associated with the electron-transit-time effects, the plasma instability leading to the self-excitation of the plasma oscillations (and the emission of terahertz radiation) becomes feasible when the dc current (photocurrent) exceeds a certain threshold value. Our model explains the following experimental facts [1–3]:

(1) the threshold behavior of the plasma oscillations self-excitation and terahertz emission;
(2) similar behavior of the devices with substantially different lengths of the depleting gate but the same spacings between gates;
(3) the effect of illumination which promotes the plasma instability;
(4) the broadening of the terahertz emission spectrum as a result of the spread of the plasma frequencies of different 2DEG strips due to a dc potential drop along the channel and, hence, a difference in the electron densities electrically induced in these strips.

Acknowledgments

The authors are grateful to F T Vasko, W Knap, and Y Meziani for useful comments and information. The work was supported by a Grant-in-Aid for Scientific Research (S) from the Japan Society for Promotion of Science, Japan.

References

[1] Otsuji T, Meziani Y M, Hanabe M, Ishibashi T and Uno T 2006 *Appl. Phys. Lett.* **89** 263502
[2] Meziani Y M, Otsuji T, Hanabe M, Ishibashi T, Uno T and Sano E 2007 *Appl. Phys. Lett.* **90** 061105
[3] Otsuji T, Meziani Y M, Hanabe M, Nishimura T and Sano E 2007 *Solid-State Electron.* **51** 1319
[4] Dyakonov M and Shur M 1993 *Phys. Rev. Lett.* **71** 2465
[5] Dyakonov M and Shur M 1996 *IEEE Trans. Electron Devices* **43** 1640
[6] Ryzhii V and Shur M 2001 *Japan. J. Appl. Phys.* **40** 546
[7] Ryzhii V, Satou A and Shur M S 2005 *Phys. Status Solidi* a **202** R113
[8] Ryzhii V, Satou A and Shur M S 2006 *IEICE Trans. Electron.* E **89** 1012
[9] Ryzhii V, Khmyrova I and Shur M 2002 *J. Appl. Phys.* **91** 1875
[10] Ryzhii V, Khmyrova I, Satou A, Vaccaro P O, Aida T and Shur M 2002 *J. Appl. Phys.* **92** 5756
[11] Satou A, Ryzhii V, Khmyrova I, Ryzhii M and Shur M 2004 *J. Appl. Phys.* **95** 2084
[12] Otsiji T, Hanabe M and Ogawara O 2004 *Appl. Phys. Lett.* **85** 2119
[13] Shockley W 1938 *J. Appl. Phys.* **9** 635
[14] Ramo S 1939 *Proc. IRE* **27** 584
[15] Ryzhii V and Khrenov G 1995 *IEEE Trans. Electron Devices* **42** 166
[16] Shik A Y 1975 *Sov. Phys.—JETP* **41** 932
[17] Tkach Y Ya 1975 *Sov. Phys.—Semicond.* **9** 704
[18] Ryzhii V, Ryzhii M and Liu H C 2002 *J. Appl. Phys.* **91** 5887
[19] Shik A Y 1995 *Electronic Properties of Inhomogeneous Semiconductors* (Luxemburg: Gordon and Breach)
[20] Ryzhii V 1997 *J. Appl. Phys.* **81** 6442
[21] Ryzhii V and Liu H C 1999 *Japan. J. Appl. Phys.* **38** 5815
[22] Ryzhii V, Ryzhii M and Liu H C 2002 *J. Appl. Phys.* **92** 207
[23] Ryzhii M, Ryzhii V, Suris R and Hamagichi C 2000 *Phys. Rev.* B **61** 2442
[24] Ryzhii V, Khmyrova I, Ryzhii M, Suris R and Hamagichi C 2000 *Phys. Rev.* B **62** 7268
[25] Dyakonov M I 2008 *Preprint* 0802.3780 [cond-mat]
[26] Kustov V L, Ryzhii V I and Sigov Yu S 1980 *Sov. Phys.—JETP* **52** 1207
[27] Bannov N A and Ryzhii V I 1982 *Sov. Phys.—Semicond.* **17** 439
[28] Shiktorov P, Starikov E, Gruzinskis V, Varani L, Palermo C, Millithaler J-F and Reggiani L 2007 *Phys. Rev.* B **76** 045333